universität wien

MASTERARBEIT | MASTER'S THESIS

Titel | Title

Reconstitution of ISG15 and its conjugation machinery to study the effects of ISGylation on the proteome during viral infection

verfasst von | submitted by

Miriam Theresa Philipp BSc

angestrebter akademischer Grad | in partial fulfilment of the requirements for the degree of

Master of Science (MSc)

Wien | Vienna, 2024

Studienkennzahl lt. Studienblatt | Degree programme code as it appears on the student record sheet:	UA 066 830
Studienrichtung lt. Studienblatt | Degree programme as it appears on the student record sheet:	Masterstudium Molecular Microbiology, Microbial Ecology and Immunobiology
Betreut von | Supervisor:	Dipl.-Biochem. Dr. Marco Yannic Hein

Abstract

The innate immune response is the first line of defense against invading pathogens. Once the pathogen is sensed, infected cells secrete cytokines such as interferons, which trigger a transcriptional response in cells in the surroundings. One of the genes that the type 1 Interferon response induces most strongly and quickly is interferon stimulated gene 15 (ISG15). The protein consists of two ubiquitin-like domains connected by a hinge region and was initially found due to its cross-reactivity with anti-ubiquitin antibodies. While ISG15 only shares about 30% sequence homology with ubiquitin, the C-terminal amino acid motif, "LRLRGG" is conserved, allowing the protein to establish covalent isopeptide bonds with its target substrates, in a process termed ISGylation. Similar to ubiquitination, conjugation of ISG15 to its target proteins requires a cascade of three enzymes, in humans, these are: UBA7, an ATP-dependent E1 activating enzyme, UBE2L6 as the E2 conjugating enzyme, and one of three E3 ligases, HERC5, TRIM25, and ARIH1.

Given that the Interferon pathway induces ISG15, it has been suggested that both ISGylation and ISG15 contribute to the host's defense against viral infection. To fully characterize the impact of ISGylation during viral infection, a proteome-wide approach is necessary, as previous studies mostly examined the effects of ISGylation on individual host and viral proteins. Studying ISGylation specifically presents additional challenges since it impacts a wide range of host proteins, particularly those other proteins that are produced in response to Interferon signaling.

Thus, it was our objective to engineer a system where ISGylation can be disentangled from the global Interferon response. First, plasmids containing the sequences of all components of the ISGylation machinery were designed. The genes for ISG15 and the E1, E2, E3 enzymes were cloned into lentiviral vectors, which were then used to generate cell lines inducibly expressing the ISGylation machinery via the TetOn system. ISG15 was cloned in variants that are either tagged with V5 or untagged, and conjugation competent or conjugation deficient,

because of mutations in the “LRLRGG” motif. To model endogenous ISGylation levels we tested multiple time points of induction for the TetOn system. Furthermore, we showed that the Interferon response could be effectively shut down with the JAK inhibitor Ruxolitinib, with the idea of suppressing the global response generally while inducing the ISGylation machinery specifically.

These engineered cell lines can be used for whole proteome analysis to gain more insight into the specific effects of ISGylation on the human proteome without the context of a general interferon response. Moreover, our ISG15 constructs are fused to a V5 tag to enable pulldown assays enriching for ISGylated proteins. The cells will also be used to identify viral ISGylation substrates.

Acknowledgements

I would like to thank the Baccarini and the Versteeg Labs for providing most of the plasmids that were used during this project. Furthermore, I want to thank the entire Hein Lab for their continuous support over the past year. I want to thank Leon Schmidt for providing me with gossip and romanian chocolate and Sebastian Platzer for his wisdom (“sucks to suck”), but seriouly I am very grateful for the community that we have in the lab! I also want to thank Marco Hein for not only coming up with the project but also guiding me through each step in our weekly meetings and helping me stay positive when things were not working. I also want to thank him for his help during the writing of this thesis. Most of all I want to thank my direct supervisor Kavya Shetty who not only provided me with the resources to be able to do this project and the data from her own experiments, but also supported me during the entire time in the lab with her knowledge and advice. She taught me so much but also gave me enough space to learn how to figure things out myself. In total I learned so much this past year (ATG are three very important letters), and I will miss the Hein Lab a lot!

Introduction

When a cell is invaded by a pathogen for example a virus, molecular components of the invader such as nucleic acids are recognized by pattern recognition receptors (PRRs), these receptors can then activate downstream signaling cascades that serve to protect the cell during infection (Dalskov et al., 2023). One such PRR is retinoic acid inducible gene I (RIG-I). Upon recognition of a nucleic acid molecule the receptor releases signaling domains which interact with mitochondrial antiviral-signaling protein (MAVS), which activates various transcription factors such as Interferon regulatory factor 3 (IRF3). The transcription factor migrates to the nucleus and binds to certain genomic sequence motifs termed Interferon sensitive response elements (ISRE). This induces the transcription of type I Interferons (IFN-α and IFN-β) (Thoresen et al., 2021). These cytokines then act as paracrine signaling molecules and bind to Interferon receptors (IFNAR) on neighboring cells. The activation of this receptor enables the phosphorylation and dimerization of Signal transducer and activator of transcription STAT1 and STAT2 via the IFNAR associated JAK1 and TYK2 kinases. The STAT heterodimer then migrates to the nucleus where it associates with Interferon regulatory factor 9 (IRF9) to form the transcription factor Interferon stimulated gene factor 3 (ISGF3). Through the binding of ISGF3 to the ISREs, transcription of Interferon stimulated genes (ISGs) is upregulated (Platanitis et al., 2019). Among the most strongly and rapidly induced ISGs is *ISG15* which encodes a ubiquitin-like protein of the same name. ISG15 is 17-kDa large in its nascent form but through proteolytic cleavage the 15-kDa mature protein is produced (Potter et al., 1999).

ISG15 was first discovered because it cross-reacted with antibodies against ubiquitin and was previously named ubiquitin cross-reactive protein (UCRP). It has 30% sequence homology to ubiquitin and consists of two ubiquitin-like domains that are connected by a short linker also called hinge region. Furthermore, it contains the ubiquitin C-terminal amino acid motif “LRLRGG” which is exposed after proteolytic processing of the nascent protein and enables covalent conjugation

of target substrates. This covalent bond is formed with a lysine residue on its target protein and is referred to as ISGylation. In contrast to ubiquitination, ISGylation is not generally considered as a tag for degradation by the proteasome. Another key difference is that ISG15 has not been shown to self-conjugate and form chains like ubiquitin (Narasimhan et al., 2005).

ISG15 is very rapidly induced but there is an approximate 12 hour delay between Interferon treatment and ISGylation, that is because like in ubiquitination three enzymes are needed to facilitate conjugation of ISG15 to its target proteins, these three enzymes together are termed the ISGylation machinery (Mirzalieva et al., 2022). The E1 activating enzyme is called UBA7 in humans and forms a thioester bond between its catalytic cysteine and the C-terminal carboxyl group of ISG15 in a ATP-dependent manner (Afsar et al., 2023). ISG15 is then transferred to the E2 conjugating enzyme UBE2L6 via trans-thiolation and later to one of three E3 known ligases which catalyzes the covalent isopeptide bond between ISG15 and the lysine on its target protein. ISGylation is reversible by the deISGylase USP18. The E1 enzyme UBA7 is specific to ISG15 only, whereas UBE2L6 can also act as E2 enzyme for ubiquitin, however it has been shown to have a much higher affinity for UBA7 than the ubiquitin specific UBA1 (Sandy et al., 2020). There are three known E3 ligases for ISG15: HERC5 (HECT and RLD containing E3 ubiquitin ligase 5), TRIM25 (tripartite motif protein 25), and ARIH1 (ariadne-1-homolog), with each of them also having ubiquitylation capabilities. Additionally, each ligase conjugates ISG15 to its substrates in a distinct manner. While HERC5 facilitates ISGylation via a HECT domain, TRIM25 is a Really interesting new gene (RING) ligase and ARIH1 is a RING-HECT hybrid (Xiong et al., 2022). There is currently little known about the target specificities of each of the E3 ligases. However, HERC5 has been shown to associate with polysomes which is why it is hypothesized that ISGylation occurs in a co-translational manner (Durfee et al., 2010).

ISG15 modifies a myriad of host proteins and impacts their function. One example is ISGylation prolonging the activated state of STAT1 whose signaling leads to the transcription of ISGs. However, ISGylation of the double-stranded RNA sensor RIG-I

leads to a downregulation of the Interferon response by reducing its cytosolic level through autophagic degradation. It has also been shown that RIG-I stabilizes the mRNA of the E3 ligase TRIM25, which leads to an increase of ISGylation (Wu et al., 2020). ISGylation of MDA5 is needed for the cell to mount a correct Interferon response. Another nucleic acid sensor has been shown to be ISGylated, namely cyclic GMP-AMP synthase (cGAS). In contrast to the ISGylation of RIG-I, the enzymatic activity of cGAS is potentiated as the conjugation with ISG15 mediated by HERC5 promotes the proteins oligomerization in the presence of DNA (Chu et al., 2024), ARIH1 has also been shown to facilitate ISGylation of cGAS (Xiong et al., 2022). The Stimulator of Interferon Response Gene (STING) is imperative for the induction of the Interferon pathway during a viral infection. The ISGylation of this protein prevents its degradation and thus leads to the upregulation of type I Interferons (Qin et al., 2024). In summary, ISG15 modifies many of the key players in the cell's response to infection, hereby it can act as a positive as well as negative regulator of the Interferon pathway.

Because ISG15 is induced by the Interferon pathway it was proposed that ISG15 and ISGylation play a role in the host defense against viral infection and it has been shown in various studies that viral proteins are ISGylated including the NS1 of Influenza A (IAV), NP of Influenza B (IBV), the VP40 of Ebola virus or the Gag protein of HIV. Conjugation of ISG15 has various antiviral effects like ISGylation of the IAV NS1 hindering the nuclear translocation of the protein (Zhao et al., 2010). ISGylation of the IBV NP prevents its oligomerization, this disturbs viral RNA synthesis (Zhao et al., 2016). Similarly, ISG15 conjugation to the Ebola virus VP40 prevents the budding of virus-like particles from the host cell (Okumura et al., 2008). Furthermore, the E3 ligase HERC5 associates with the HIV gag protein and halts the assembly of gag particles at the membrane (Woods et al., 2011). However, contrasting to the above described activities, ISG15 also has pro-viral effects in some cases like facilitating the egress of Vaccinia virus (VACV) virions (Bécares et al., 2023).

Viruses have also developed countermeasures against ISG15 further highlighting the importance of the protein during infection. The human cytomegalovirus (HCMV)

pUL26 for example inhibits the ISGylation of cellular proteins and the IBV NS1 sequesters ISGylated NP, counteracting the modification's antiviral effect. (Perng & Lenschow, 2018). Coronaviruses like SARS-CoV-1/2 express PLpro which acts as a potent deISGylase. The protease removes ISG15 from the transcription factor IRF3 which leads to a downregulation of the Interferon response (Shin et al., 2020).

While ubiquitin is conserved among a wide range of species there is significant divergence between the sequence of ISG15 in different organisms, for example human and mouse ISG15 share only 63.4% sequence homology. Additionally, the function varies between the two species with ISG15 KO mice being more susceptible to viral infection whereas humans that naturally express no ISG15 do not have higher risks of viral infection (Speer et al., 2016). It was shown that this is because ISG15 stabilizes its own deISGylase USP18 through non-covalent interaction (Zhang et al., 2014) and USP18 is a prominent negative regulator of the Interferon response, as it can displace JAK1 (Arimoto et al., 2017). Thus, patients lacking ISG15 have more activation of the Interferon pathway and are more prone to dermatologic inflammation (Martin-Fernandez et al., 2020) and mycobacterial diseases (Bogunovic et al., 2012). On the other hand, ISG15 null mice have not been shown to exhibit autoinflammation. The susceptibility to mycobacterial disease in patients lacking ISG15 also stems from the fact that unconjugated ISG15 can be secreted and lead to the upregulation of IFN-γ production, which is essential for antibacterial immunity (Bogunovic et al., 2013).

While many targets of ISG15 have been identified, these substrates were largely studied in isolation and since ISGylation is a proteome wide phenomenon a system's level approach is needed to fully comprehend its effects. Most of the proteomic studies of ISGylation have identified less than 100 substrates of ISG15 (Thery et al., 2021). Although one group identified 476 targets of ISGylation, they used Interferon treatment to stimulate the cell and not a viral infection, thereby they only looked for host proteins (Pinto-Fernandez et al., 2020). Another group performed a proteomic study using A549 cells infected with Influenza A virus, however only 22 substrates of ISG15 were analyzed here (Peng et al., 2016).

Moreover, many ISGs are ISGylated themselves (Zhao et al., 2005), which makes it difficult to detect viral proteins in a mass spectrometry (MS) analysis because they are much lower in abundance than the host proteins. Therefore, we want to isolate ISGylation from the general Interferon response.

To study the function of ISG15 and ISGylation of its targets in a reductionist fashion, isolated from the general effects of the interferon response, we engineered cell lines where the ISGylation machinery can be induced individually, without a global interferon response, which can be suppressed pharmacologically with the potent Janus kinase inhibitor Ruxolitinib (Ostojic et al., 2011). To this end, vectors for inducible recombinant expression of ISG15 and its machinery were designed. These plasmids were then used to produce lentivirus and later transduce A549, which are human epithelial lung cancer cells, to obtain cell lines expressing the ISGylation machinery. Furthermore, the system is doxycycline (Dox) inducible via the TetOn system, which has shown high sensitivity and low basal gene expression “leakiness” (Das et al., 2016). The inducible expression will hopefully allow us to more closely model endogenous ISG15 expression during a viral infection.

Results

Inhibition of the Interferon response

Theoretical part

In order to investigate the functions of ISGylation fully it needs to be disentangled from the global Interferon response. To shut down the type I Interferon response there are two options, the first one being generating a Interferon receptor (IFNAR) KO cell line. This method would have the advantage that once it is confirmed that the Interferon receptor is no longer functional nothing else needs to be added to the cells. However, creating a knockout cell line involves cloning and transfection steps that might entail a lot of trial and error. Furthermore, the IFNAR knockout cells might be able to induce the production of ISGs through alternative pathways.

The second option is to pharmacologically inhibit the Interferon response by blocking one or multiple of the proteins involved in this pathway. While this method offers only a transient inhibition it is a less time-consuming option. For this project, the second option was chosen and the small molecule inhibitor Ruxolitinib was used to block the Interferon pathway.

Ruxolitinib is a drug that inhibits Janus kinases which mediate signal transduction from the cell surface to the nucleus during the Interferon response. Therefore it should inhibit the downstream expression of ISGs, including ISG15. The chemical has been shown to inhibit Janus kinases with an IC_{50} value (half-maximal inhibitory concentration) of 3.3 nM for JAK1 and 2.8 nM for JAK2. Furthermore, it was found that Ruxolitinib selectively inhibits Janus kinases, having no effect on kinases not involved in the Interferon pathway. The IC_{50} for STAT3 phosphorylation which was used as a proxy for the inhibition of the JAK/STAT pathway was calculated to be about 280 nM in whole blood. (Quintás-Cardama et al., 2010).

Ruxolitinib isn't just used for blocking the global Interferon response in cell culture, but it also has various applications in the clinic. For example the JAK inhibitor has

been used to treat myelofibrosis, a condition where patients present a chronically activated JAK-STAT pathway, which leads to bone marrow disease (Ostojic et al., 2011).

Results

Our goal was to establish a protocol to be able to separate ISG15 and ISGylation from the global Interferon response using pharmacological inhibition.

This was tested by using an A549 cell line that has the sequence of the fluorescent protein mCherry fused to an Interferon sensitive response element (ISRE), which means that when the cells are treated with IFN-β, mCherry is expressed. However, when the Interferon pathway is disrupted by inhibiting Janus kinases there should be no or at least much less mCherry expression (Figure 1a).

The following concentrations of Ruxolitinib were used: 0.02, 0.2, 1, 2, 5, 10 μM. Additionally, there was one positive control where no Ruxolitinib was added but the cells were treated with Interferon, here the maximum of mCherry expression was expected. Furthermore, one negative control was prepared, these cells were not treated with Ruxolitinib or Interferon.

After pretreating the cells with Ruxolitinib for 2 hours, IFN-β was added to the medium, the following day the cells were analyzed for mCherry expression using Flow Cytometry. The results of the FACS analysis showed that Ruxolitinib did decrease the expression of mCherry with increasing concentrations of the small molecule inhibitor. A direct comparison of the cells treated with the different concentrations of Ruxolitinib showed a clear shift in the population from the positive control to 0.2 μM (Figure 1b).

The FACS analysis showed 3.65 % mCherry positive cells in the cells that were not treated with Ruxolitinib but stimulated with Interferon compared to only 1.36 % positive cells in the sample treated with the lowest concentration of Ruxolitinib (0.02 μM), this corresponded to about 50 % inhibition. There was almost complete

inhibition at 0.2 µM with only 0.04% mCherry positive cells. At 1 µM and higher concentrations the inhibition plateaued and the mCherry levels were comparable to that of the negative control (Figure 1c)

In conclusion, we were able to show that Ruxolitinib sufficiently inhibits Interferon signaling at concentrations as low as 200 nM which is also consistent with the literature. This concentration of the inhibitor will also be used for further experiments to suppress the Interferon response for example during viral infection.

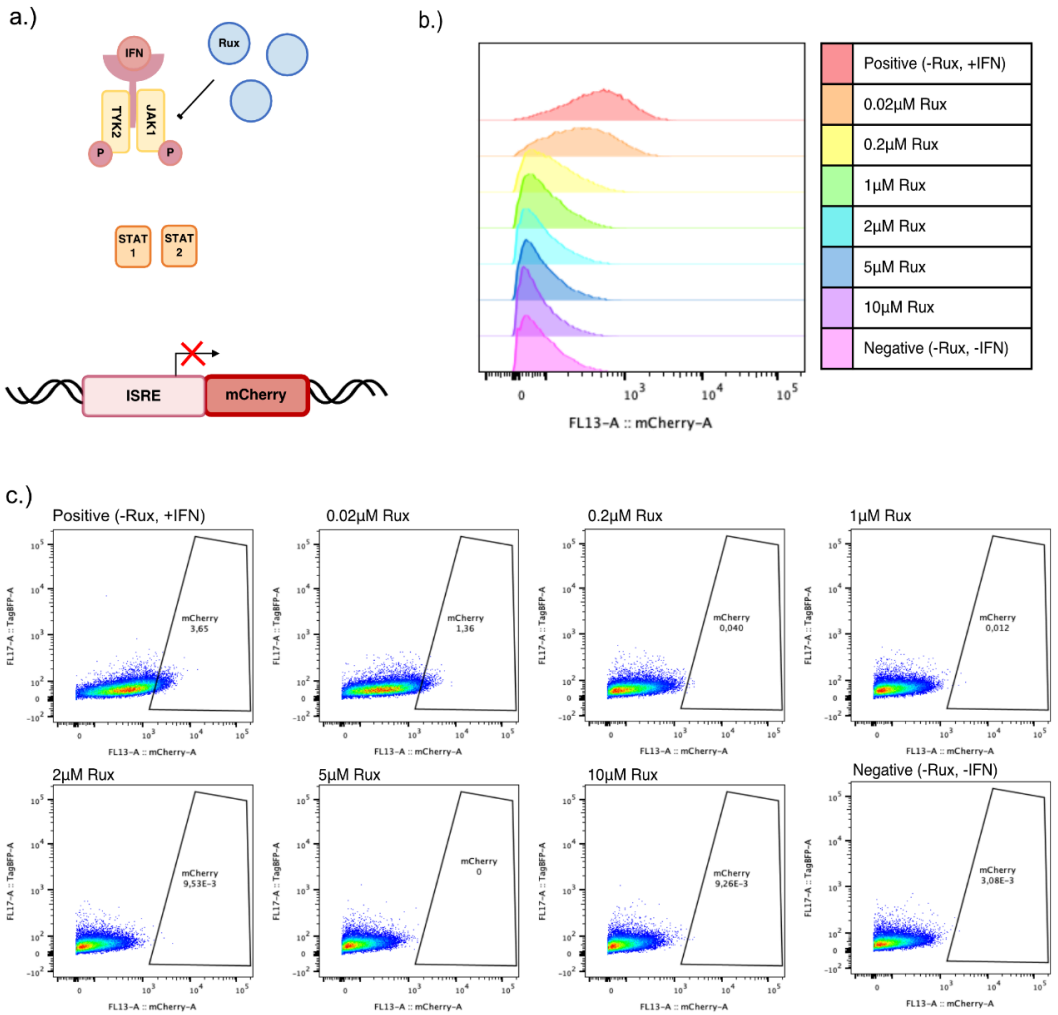

Figure 1 Inhibition of the Interferon response: **a.)** cell line with ISRE fused to mCherry to test Interferon pathway inhibition; **b.)** FACS data for cells treated with different Ruxolitinib concentrations; **c.)** percentage of mCherry positive cells, from left to right: positive control, 0.02, 0.2, 1, 2, 5, 10 µM Ruxolitinib treatment, negative control

Cloning strategy

Theoretical part

In order to create a cell line exogenously expressing ISG15 and the three enzymes needed for conjugation one strategy would be to clone each of the genes of interest separately into a plasmid. However, transfecting four plasmids is time-consuming and stressful for the cells, so in this project, we looked for a strategy to reduce the amount of transfections. Because all four genes in one plasmid would be too big for a lentiviral transfection the ISG15 expression machinery components were split in two plasmids, the first construct containing ISG15 and the E1 enzyme UBA7 and the second construct containing E2 UBE2L6 and one of the E3 ligases (HERC5, TRIM25, and ARIH1). This cloning strategy was inspired by Nakashima et al., 2015 who cloned the ISGylation machinery into the Gateway cloning vectors pLenti CMVTRE3G Neo DEST and pLenti CMVTRE3G Puro DEST. However, with the information on the primers given in the paper, we were not able to replicate their cloning strategy in silico. Therefore we decided to use Gibson assembly to create the constructs and designed new primers, as the reagents for Gibson assembly were readily available and more cost-effective compared to Gateway cloning.

Gibson assembly is a molecular cloning method that was first described in 2009 and allows the assembly of constructs that are several hundred kilobases in size without the need for restriction enzyme sites. The genes of interest and the vector are first PCR amplified with primers that contain 30-60 nucleotide overlaps to the neighboring fragment. After the amplification the entire assembly is done in an isothermal reaction at 50 °C that takes 15-60 minutes depending on the number of fragments. During the reaction the ends of the fragments are first digested by a 5’-exonuclease. The complementary overlaps can then anneal and the gaps are filled in by Phusion polymerase. Lastly, the nicks in the double strand are sealed by Taq ligase (Gibson et al., 2009).

As the vector for the ISGylation machinery pCW57.1 was used. This is a lentiviral expression plasmid that can be used as a Gateway destination vector but for this

project, it was used for Gibson assembly. This plasmid contains a tight TRE promoter as well as the rtTA-advanced transactivator for doxycycline inducible expression of the gene of interest. Furthermore the vector contains the gene for puromycin N-acetyl-transferase, making the cells that are transfected with the plasmid resistant to the antibiotic puromycin.

As two constructs were designed to exogenously express the ISGylation machinery, puromycin resistance was used as a selection marker for the construct containing the E2 and E3 enzymes. For the plasmid containing ISG15 and the E1 enzyme EGFP was used as a selection marker. This is a fluorescent protein with an excitation wavelength of 488 nm and an emission wavelength of 507 nm, that was originally isolated from the jellyfish *Aequorea victoria*. Both selection marker genes are under the regulation of a constitutive phosphoglycerate kinase 1 promoter (PGK).

There are 4 versions of ISG15 that were used for this project namely V5-ISG15, V5-ISG15^{AA}, ISG15 and ISG15^{AA} the latter two will be used as negative controls for immunoprecipitations using the anti-V5 antibody to account for nonspecific binding of the beads used for the pulldown. The conjugation-deficient variant of ISG15 is referred to as ISG15^{AA} and will serve as a control for non-covalent interactions of ISG15 with other proteins in mass spectrometry experiments. Instead of the Gly-Gly motif that is needed for conjugation, it has two alanine residues which makes it incapable of covalently conjugating with lysine on ISG15 substrates. The V5 tag on ISG15 can be used for later immunoprecipitation experiments as there exists a widely used and sensitive antibody against V5.

The sequences of ISG15 and the E1 enzyme as well as the E2 and E3 enzymes are connected using P2A. 2A peptides induce ribosomal skipping because of the conserved amino acid sequence GDVEXNPGP at the C-terminus of the peptide. These peptides are used to express two or more genes under the same promoter without creating a fusion protein as the two proteins get separated during translation. All 2A peptides were isolated from viruses, for example, P2A was

discovered in the porcine teschovirus. There are also multiple other 2A peptides from different viruses like F2A from foot-and-mouth disease virus, but P2A is the most effective concerning polycistronic gene expression (Liu et al., 2017). At the beginning of the 2A sequence the three amino acids “GSG” were added as this increases the efficiency of the ribosome skipping process.

Another reason why P2A was chosen for the polycistronic expression of the components of the ISGylation machinery is that on the same plasmid, the gene for puromycin resistance is connected to the rtTA transactivator via a T2A peptide. As the plasmid is a lentiviral vector and lentivirus tends to recombine homologous sequences it was decided to use two different 2A peptides.

Because the P2A is cleaved at the proline amino acid located at the C-terminus, approximately 20 amino acids remain on the upstream protein, which would be ISG15 in this case. Since the ability to form covalent bonds with its targets is mediated by the Gly-Gly on the C-terminus, another sequence was added between the Gly-Gly and the P2A, the carboxyl-terminal “GTEPGGRS” extension. This extension is also found on newly translated endogenous ISG15 and prevents degradation of the pro-ISG15 precursor protein. The extension is cleaved by a 100 kDa protease. The activity of the protease is independent of the induction of the Interferon pathway. This enzymatic cleavage generates the mature ISG15 by exposing the “LRLRGG” motif necessary for covalent conjugation (Potter et al., 1999).

Results

The aim of the cloning strategy was to clone the entire ISGylation machinery as effectively as possible. The plasmids were designed using the pCW57.1 backbone and all of them include the TetO, however only the constructs containing the E2 and E3 enzymes contain the rtTA transactivator. Since all cells will be transduced with a lentivirus containing an ISG15 variant and the E1 as well as another lentivirus containing the E2 and one of the E3 ligases, it is sufficient for the transactivator to be present on one of the two constructs. All plasmids were designed to have the TetO followed by the two genes of interest connected by a P2A sequence followed by a selection marker under the constitutive promoter PGK. The sequences for the components of the ISGylation machinery were PCR amplified from plasmids provided by the Versteeg Lab except for TRIM25 and ARIH1 which were amplified from HeLa cDNA. All plasmids were then cloned via Gibson assembly and named pMP001-7 with pMP001-4 containing the E1 enzyme and either V5 tagged or untagged ISG15 that is either conjugation competent ($ISG15^{GG}$) or incompetent ($ISG15^{AA}$) and pMP005-7 containing the E2 enzyme as well as HERC5, TRIM25, or ARIH1 (Figure 2a). The sequences of the constructs were deduced by nanopore sequencing performed by the company Plasmidsaurus. It was confirmed that pMP001-5 contain no nucleotide changes in coding regions that could cause an amino acid change.

The sequencing results showed that TRIM25 has a mutation at the amino acid position 358 which changes the proline to a leucine, compared to the reference genome. This appears to be a feature of the template which is cDNA from HeLa cells (Figure 2b). AlphaFold modeling indicates that this position is in an unstructured region. Therefore, we decided to go ahead with this version of the gene. However, this needs to be kept in mind in case later on there are discrepancies between the expected and actual function of the protein.

The ARIH1 nucleotide sequence contains an about 100 base pair long region that has almost 90 % GC content. During a PCR this is almost impossible to amplify for the polymerase, it just creates a deletion in this region. This is why we were

unfortunately not able to obtain a PCR product for the entire ARIH1 sequence and thus could not clone it into a lentivirus plasmid (Figure 2c). After two failed attempts at cloning ARIH1, it was decided to stop efforts to generate this plasmid until we could find a way to clone it without PCR amplification.

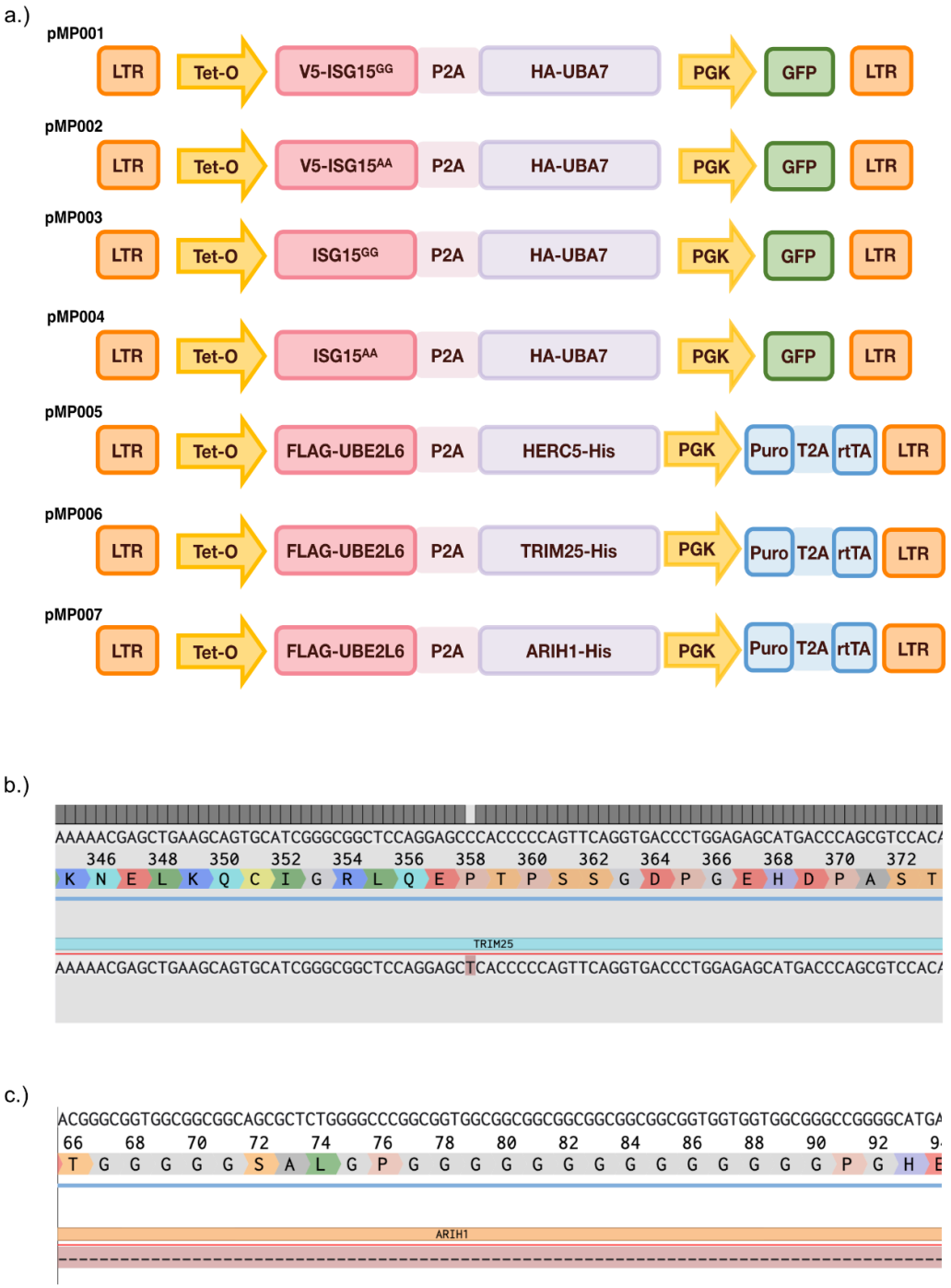

Figure 2 Cloning strategy: **a.)** all sequences between the LTRs of the engineered plasmids, from top to bottom pMP001, pMP002, pMP003, pMP004, pMP005, pMP006, pMP007; **b.)** point mutation in TRIM25 plasmid; **c.)** nucleotide stretch in ARIH1 sequence with 90% GC content

Cell line generation and selection

Theoretical part

Our aim was to create cell lines where the ISGylation machinery is stably integrated into the cell's genome. To this end, we used lentivirus to deliver the genes of interest. The lentivirus gene delivery system is derived from the human immunodeficiency virus (HIV) which is a retrovirus. This system is a convenient option to exogenously express genes of interest and has been in use for decades.

As the lentivirus gene delivery system was derived from a pathogenic virus, efforts have been made to address biosafety concerns. For this project the third generation lentivirus system was used. This encompasses two packaging plasmids, one of them contains *Gag*, which encodes three viral core proteins: the matrix protein, the capsid protein, and the nucleocapsid protein. It also contains *Pol*, which encodes the viral protease, the reverse transcriptase, and integrase. The other packaging plasmid encodes *Rev* (regulator of expression of virion proteins), which binds to Rev-response elements (RRE), which subsequently leads to the export of viral RNA. Additionally, there is an envelope plasmid that encodes the VSV glycoprotein, giving the lentivirus broad tropism. The fourth plasmid contains one or multiple genes of interest between the two long-terminal repeats (LTRs). The third-generation lentivirus does not need the HIV *Tat* gene which is a transactivator. This fact and having *Gag* and *Pol* encoded by two separate plasmids enhanced the biosafety of lentiviral gene delivery (Dull et al., 1998).

Results

A549 were chosen as the background cell line for the reconstitution of the ISGylation machinery as they have low basal expression of ISG15 and high amounts of ISGylation upon Interferon stimulation. This was shown in a Western blot using an anti-ISG15 antibody done by Kavya Shetty. Here, multiple cell lines were used to compare ISG15 expression and ISGylation of the cells without treatment or after IFN-β stimulation (Figure 3a). Furthermore, this cell line is permissive to viral infection and is especially suitable for studying respiratory viruses as it is an epithelial lung cancer cell line. Previous studies have also used this cell line to investigate the effects of ISGylation on the proteome.

Firstly, the lentivirus was made of pMP001-6 as described in the Methods section, the lentivirus made from these plasmids will be referred to as LnMP001-6. To produce lentivirus HEK293T cells were used. The plasmids pMP001-4 contain GFP, which was visible in the HEK293T cells producing the lentivirus as shown by a confocal microscope image of cells transfected with pMP001 (Figure 3b).

After collection of the lentiviral supernatant, A549 cells were transduced with a lentivirus containing one of the ISG15 variants. It was suspected that the lentiviral titer would be low because of the size of the plasmids, so a mixture of 50 % lentiviral supernatant and 50 % cell culture medium was used to achieve the highest yield of positive cells. The selection marker for these cells was GFP. About 48 hours after the transduction the cells were analyzed to deduce the percentage of GFP-positive cells. The amount of GFP-positive cells was 3.5 % for LnMP001, 7.5 % for LnMP002, 14.7 % for LnMP003, and 10.3 % for LnMP004 (Figure 3c). Additionally, HEK293T was transduced with the same lentiviruses to compare the infection rate of the two cell lines (Figure 3d). It was observed that the transduction efficiencies were similar across the two cell lines with 4-14 % GFP positive cells for the transduced HEK293T. Therefore, it was then decided to continue the experiments with A549. The transduced A549 were sorted for GFP-positive cells using flow cytometry and cultured until they could be transduced with either

LnMP005 or LnMP006. These cells were then selected with the antibiotic puromycin as the cells containing the lentivirus should express a puromycin resistance gene. The puromycin selection was started 48 hours after the transduction by adding 3 µg/mL of the antibiotic to the medium. After 48-72 hours most of the cells in the non-transduced negative control were dead and small colonies of resistant cells were forming in the transduced populations. The resistant cells were further cultured in 1 µg/mL puromycin to remove any cells where the PGK promoter was silenced.

Additionally, A549 had previously been transduced with either LnMP005.1 or LnMP006.1 to integrate the E2 and E3 enzymes into the genome, the cells containing the genes of interest were then selected for with puromycin. These lentiviruses were made of a previous version of pMP005 and pMP006 that lack a stop codon on the E3 enzyme. Even though the constructs were not completely correct the cells were not discarded because they could be used for preliminary experiments. These cells were then transduced with LnMP001 and LnMP002 and GFP positive cells were sorted by FACS. Here the transduction efficiency was slightly lower compared to A549 with 2.8 % positive cells for LnMP001 and 5.2 % for LnMP002 (Figure 3e).

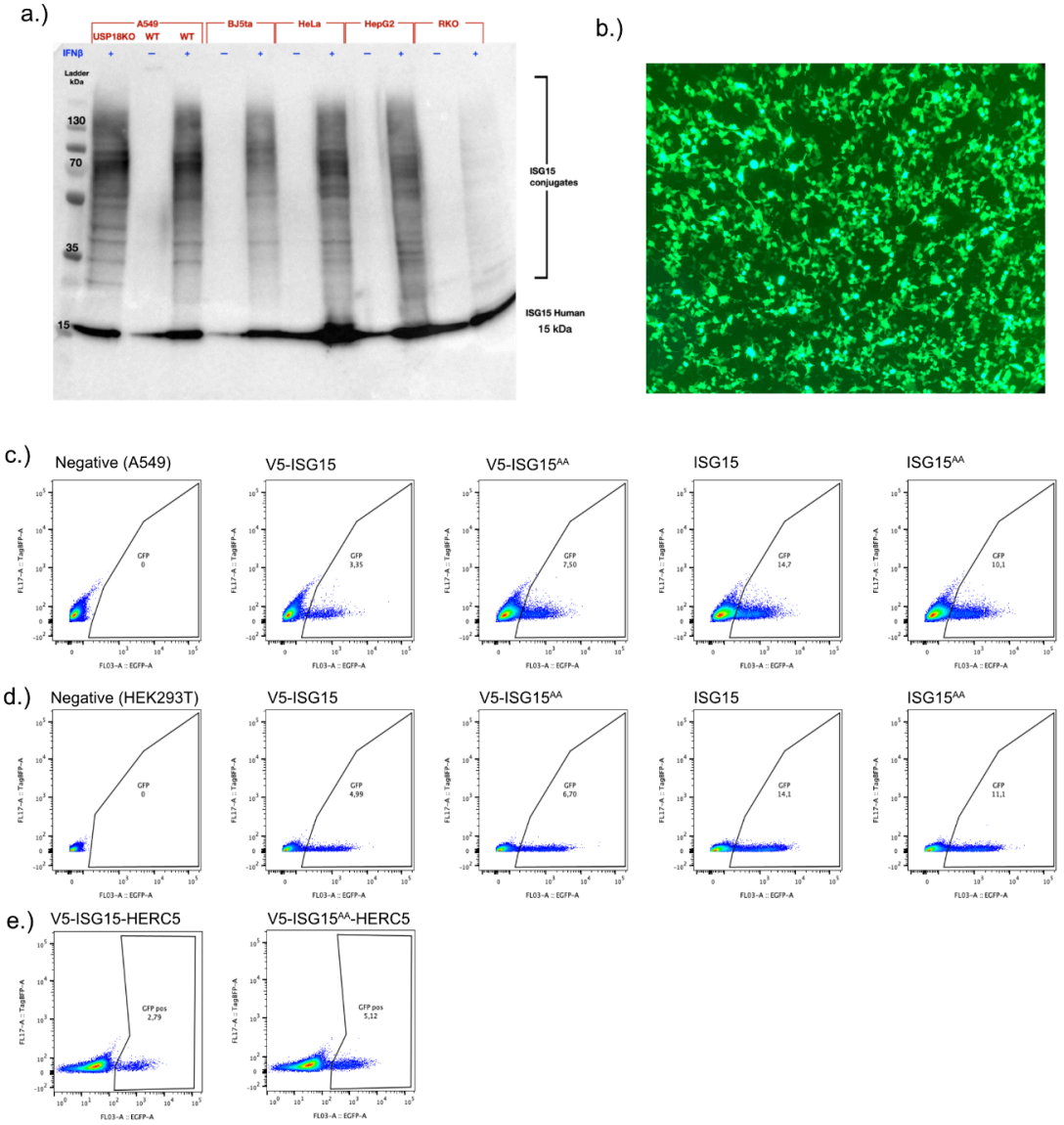

Figure 3 Cell line generation and selection: **a.)** Western blot showing ISGylation pattern of cells different cell lines either treated with IFN or not, using ThermoFisher ISG15 antibody, experiment done by Kavya Shetty; **b.)** confocal microscope image of HEK293T transfected with pMP001; **c.)** percentage of GFP positive cells in A549 transduced with (from left to right) negative, LnMP001, LnMP002, LnMP003, LnMP004; **d.)** percentage of GFP positive cells in A549 transduced with (from left to right) negative, LnMP001, LnMP002, LnMP003, LnMP004; **e.)** percentage of GFP positive cells of cMP0016 transduced with LnMP001 and LnMP002 (from left to right)

Inducible expression

Theoretical part

As ISGylation is induced by the Interferon response we were looking for a system where we could model this inducible expression without having to stimulate the cells with Interferon. There are a few different types of inducible expression systems such as the Lac-operator-repressor system, the cumate-controlled operator system, and the tetracycline-controlled operator system (Kallunki et al., 2019). The tetracycline-controlled operator system was chosen for this project as the “leakiness” (expression of the transgene in the absence of the inducer) is low and the sensitivity to the inducer is high.

The Tet operon was first discovered in Gram-negative bacteria and it encodes the membrane protein TetA which facilitates the efflux of the antibiotic tetracycline. Since even low levels of TetA can be detrimental to the cell in the absence of tetracycline its expression is tightly regulated by the tetracycline-responsive repressor TetR. This protein dimerizes and binds to the tetO regulatory elements which leads to the suppression of the promoters of both TetA and TetR. In the presence of tetracycline or one of its derivatives, a conformational change is induced and the TetR dimer cannot bind to the tetO regulatory region anymore, thus allowing the production of TetA, which then facilitates the efflux of the antibiotic (Bertram & Hillen, 2007).

The tetracycline-controlled operator was then engineered for application in eukaryotic cells, this was termed the TetOff system. This system enabled the repression of the transcription of the gene of interest (Gossen & Bujard, 1992). Later the TetOn system was described, in contrast to the TetOff system the expression of the gene of interest was upregulated by the addition of Doxycycline. This was made possible by introducing random mutations into the TetR gene. Through extensive screening, a TetR variant whose function was inverse to the original repressor was found. This variant was then combined with a VP16 sequence to enhance

self-transduction and was termed rtTA. In the presence of Dox this protein now activated the expression of the gene of interest (Gossen et al., 1995).

One downside of the TetOn system was that through the mutations that needed to occur to reverse the function of the repressor, it lost its original sensitivity for Dox. Through codon optimization, truncation of the VP16 sequence, and functional screening of rtTA mutants the TetOn system was improved over the years. Through these improvements, the novel rtTA became 100-fold more sensitive to Dox than the original variant (Das et al., 2016).

However, this system is not without disadvantages as the uninduced expression level can vary greatly between different cell types and the induced expression can be very different between different clones of a cell population (Rossi & Blau, 1998). Thus, it is important to check for leaky expression and to either use a polyclonal population or screen multiple clones for the desired expression levels. Furthermore, cells can lose their ability to express the transgene after multiple rounds of Dox treatment, which is why we plan to use a fresh batch of cells that haven't previously been induced for each experiment.

Results

In the TetOn system the transactivator rtTA is constitutively expressed, however as a monomer, it cannot bind the TRE promoter and induce transcription of the downstream gene. After the addition of Dox, the transactivator can then dimerize and bind the Tet operator sequences, which leads to the activation of the transcription of the gene of interest (Figure 4a). Doxycycline concentrations usually used for inducible expression range from 0.1-1 µg/mL (Das et al., 2016).

Das et al. (2016) found that after three days of Dox treatment, the induction of the gene of interest was at about 50% of the maximum, and after 5 days of the treatment the induction was at the maximum and plateaued with longer treatment (7 days). However, Heinz et al. (2013) found that after about 3 hours 60 % of the cells were induced and after 12 hours approximately 90 %, in their study the induction remained consistent after 24 hours. This discrepancy highlights the importance of testing different time points of the Dox induction. For this project, a shorter induction time is of interest as the IFN treatment to induce endogenous ISGs is done for 24-48 hours.

It is also important to note that while low concentrations of Doxycycline (0.1-1 µg/mL) do not cause cell death they do have an effect on the cell's metabolism (Ahler et al., 2013). Therefore, it is vital to find the lowest concentration of Dox at which desirable induction can be achieved.

The engineered cell lines (described in Figure 3e) containing the ISGylation machinery with HERC5 as the E3 ligase and V5-ISG^{GG} or V5-ISG^{AA} were treated with 1 µg/mL Dox for 5 days. The cells were then lysed and a Western blot was performed using the anti-FLAG-M2 antibody. The E2 enzyme UBE2L6 is tagged with FLAG, and the size of this protein with the FLAG tag is 18 kDa. There is some nonspecific binding of the antibody which can be observed in the Dox negative control, however a band can be observed between 15 and 35 kDa only in the Dox induced cells which should correspond to the FLAG tagged UBE2L6 (Figure 4b). Another Western blot was done with the anti-V5 antibody, this tag is fused to ISG15

and should yield a band at about 16.5 kDa. In the Western blot we could not observe ISGylation or an ISG15 band in the V5-ISG15 sample, the band in the V5-ISG15^{AA} could be nonspecific binding of the antibody as it corresponds to a larger protein than V5-ISG15 (Figure 4c). This could be explained by not enough protein being added to the Western blot or the incubation time of the primary antibody being too short. Further validation steps need to be performed to assess the ideal Dox concentration and time point of induction.

Furthermore, it was observed that the cell expressing WT ISG15 e.g. cMP001 grew slower compared to the cells expressing the conjugation deficient variant of ISG15 e.g. cMP002. However, there was no increase in cell death observed in the conjugation-competent compared to the non-competent populations. These observations were made even before the cells were induced with Dox.

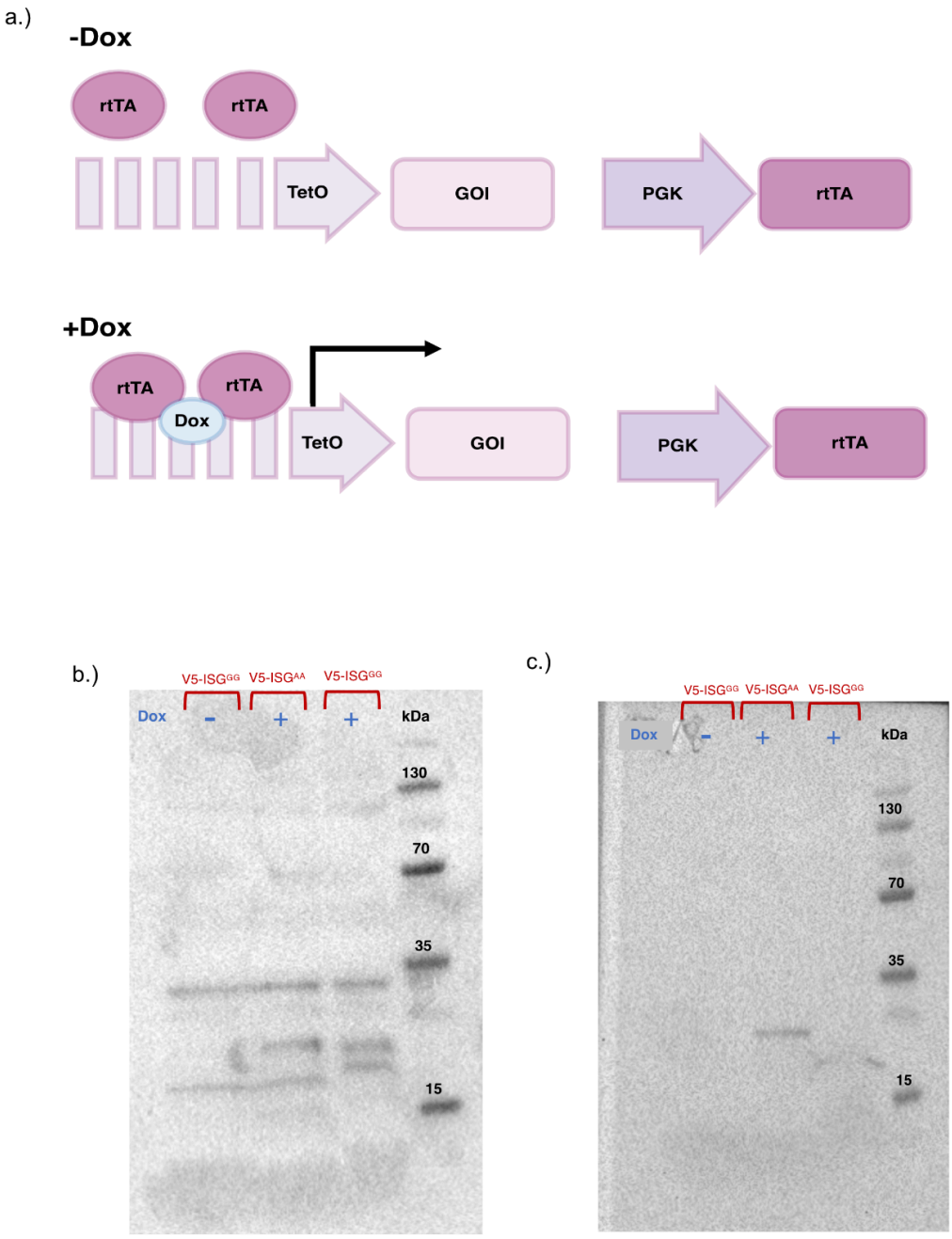

Figure 4 Inducible expression: **a.)** transcriptional activation of a gene of interest (GOI) without and with the addition of Dox; **b.)** Western blot with anti-FLAG-M2 antibody, using Dox treated or untreated cells engineered to have WT or conjugation deficient V5-ISG15; **c.)** Western blot with anti-V5 antibody using Dox treated or untreated cells engineered to have WT or conjugation deficient V5-ISG15

Methods

Cell culture

A549 and HEK293T cells were cultured in Gibco Dulbecco's Modified Eagle Medium (DMEM) with 10 % heat inactivated and filtered fetal bovine serum (FBS) and Gibco Penicillin-Streptomycin-Glutamine (PSQ). Cells were incubated at 37 ºC in 5 % CO_2 and split at 80-90 % confluency. To split the cells the medium was aspirated and washed with phosphate buffered saline (PBS) pH 7.4, PBS was then aspirated and trypsin was added to detach the cells from the plate, which was then incubated for 5 minutes at 37 °C. Trypsin was then quenched with four times the amount of medium and cells were resuspended. The desired amount of cells was then added to a new cell culture dish with the correct amount of medium according to Table 1. To thaw cells the cryovial containing the frozen cells was swirled in a 37 °C water bath until the cells were mostly thawed, they were then quickly added to a 10 cm plate with 10 mL of warm DMEM+ 10 % FBS, the subsequent day the medium was changed to remove any DMSO residue. To freeze cells, they were removed off the plate with trypsin, which was then quenched with medium. The cell suspension was then centrifuged for 5 minutes at 500 ×g, the pellet was washed with PBS and centrifuged again for 5 minutes at 500 ×g. Per one million cells 1 mL of the freezing mixture (90 % FBS and 10 % DMSO) was used to resuspend the cells, they were then aliquoted in cryovials and frozen using the Thermo Fisher Mr. Frosty™ Freezing Container in the -80 °C freezer and then transferred to the -150 °C freezer for long term storage.

Table 1: reference numbers for cell culture

Culture dish	Size (cm^2)	PBS (mL)	Trypsin (µL)	culture medium (mL)
10cm	56.7	7	1000	10
6 well	9.6	1.5	500	2
12 well	3.8	1	300	1
24 well	1.9	0.5	200	0.5
96 well	0.33	50	20	0.1

Ruxolitinib treatment

0.2 mio. A549 ISRE-mCherry (cKS0001.2) cells were seeded per well on a six-well plate the day before the experiment. Ruxolitinib was dissolved in DMSO to make a stock solution with a concentration of 20 mM (Invivogen, 2023). An aqueous dilution of 100 µM was prepared and added to the medium to achieve final concentrations of 10, 5, 2, 1, 0.2, and 0.02 µM Ruxolitinib. After 2 hours of incubation 2 µL of IFN-β were added. Hereby two wells were not treated with Ruxolitinib, one of them was later treated with IFN-β, this served as a positive control as high mCherry induction was expected here. The other well was not treated with IFN-β, serving as a negative control for the flow cytometry analysis to observe the uninduced mCherry production. The cells were subsequently incubated for 16 hours. The following day the cells were washed with PBS and prepared for flow cytometry analysis.

FACS protocol

Cells were washed with PBS (cells were washed three times if they had been treated with Lentivirus) and treated with trypsin for 5 minutes. Trypsin was then quenched with DMEM+10 % FBS and resuspended. If a higher concentration of cells was desired the cell suspension was centrifuged for 5 minutes at 500 ×g and most of the supernatant was aspirated, leaving 500 µl of medium to resuspend the cells in. The cell suspension was then transferred to a FACS tube by pushing it through the cell strainer. FACS tubes were kept on ice. Cells were analyzed with the Bio-Rad ZE5 cell analyzer (50 000 events) or sorted with the BD BioSciences FACSMelody™ cell sorter.

PCR amplification

All fragments were amplified using NEB Q5® High-Fidelity DNA Polymerase. The primers used for each of the fragments can be found in Table 2 and the PCR conditions are described in Table 3 and 4.

Table 2: amplification parameters for fragments used for the final constructs

Fragment	Origin	Length (bp)	Primer FW	Primer RV
ISG15 (V5)	#80	543	oMP0049	oMP0021, oMP0031
ISG15 (no V5)	#80	508	oMP0050	oMP0022, oMP0031
UBA7	#77	3066	oMP0032	oMP0006
PGK	pCW57.1	511	oMP0007	oMP0047
EGFP	gCH134_pCH49	717	oMP0048	oMP0010
UBE2L6	#79	483	oMP0051	oMP0033
HERC5	#86	3090	oMP0034	oMP0054
TRIM25	HeLa cDNA	1890	oMP0037	oMP0056
ARIH1	HeLa cDNA	1671	oMP0043	oMP0055
Backbone (ISG15-E1)	pCW57.1	5600	oMP0026	oMP0052
Backbone (E2-E3)	pCW57.1	7540	oMP0027	oMP0052

Table 3: PCR reaction mixture using Q5 polymerase

Component	50 µl reaction	Final concentration
5X Q5 Reaction Buffer	10 µl	1X
10 mM dNTPs	1 µl	200 µM
10 µM Forward Primer	2.5 µl	0.5 µM
10 µM Reverse Primer	2.5 µl	0.5 µM
Template DNA	variable	10 ng
Q5 High-Fidelity Polymerase	1 µl	0.04 U/µl
5X Q5 High GC Enhancer	10 µl	1X
Nuclease-Free Water	to 50 µl	

Table 4: PCR conditions in the Thermocycler using Q5 polymerase

Step	Temperature	Time
Initial Denaturation	98°C	30 seconds
35 Cycles	98°C	10 seconds
	*50–72°C	10 seconds
	72°C	20 seconds/kb
Final Extension	72°C	1-4 minutes
Hold	4°C	

NEB 6X Purple Loading Dye was added to the PCR products and they were loaded on a 1 % agarose gel with GelGreen nucleic acid stain (10 000X), 2 µL NEB 1 kb Plus Prestained DNA ladder was added and the gel was run for 20-30 minutes at 180 V. Afterwards, nucleic acid was visualized under monochromatic light to avoid mutations caused by UV imaging and DNA bands were cut out. The NEB Monarch® DNA Gel Extraction Kit was used to extract the PCR product from the agarose gel and purify them. The concentration of the extracted DNA was measured with the NanoDrop instrument. Sequences were confirmed using the Microsynth Sanger Sequencing service.

Gibson assembly

Gibson assembly was performed using the NEBuilder® HiFi DNA Assembly 2X Master Mix using either a 1:2 vector to insert ratio for reactions with one or two fragments or a 1:1 vector to insert ratio for reactions with three or four fragments. The exact amounts of each fragment and the backbone that were added to the reaction were calculated based on their length and concentration using the NEBuilder Protocol Calculator (nebuildercalculator.neb.com). 0.05 pmol of each fragment and depending on the vector to insert ratio either 0.025 or 0.05 pmol of the backbone were used in a total reaction volume of 20 µL. All reactions were incubated at 50 °C for 1 hour. Subsequently, 1 µL of the reaction was transformed into 10 µL of Takara Stellar Chemically Competent Cells. If no colonies grew on the plate 10 µL of the reaction mixture were transformed into 100 µL of the bacteria. To transform the plasmid, the reaction mixture was added to the corresponding amount of bacteria and incubated on ice for 30 minutes, the cells were then heat shocked at 42 °C for 45 seconds, they were then placed on ice again for 2 minutes. Then, SOC medium was added (10 times the volume of the bacteria) and the cells were incubated at 37 °C for one replication cycle, they were then inoculated on LB agar plates with 100 µg/ml carbenicillin and incubated overnight. For some constructs a colony PCR was done at this step to screen for the correct plasmid. To

this end the primers oMP0029 and oMP0030 together with the *Taq* 2X Master Mix were used. Multiple single colonies were inoculated in 5 mL of LB medium with 100 µg/ml carbenicillin and incubated overnight. The plasmids were then purified using the NEB Monarch Spin Plasmid Miniprep Kit. Afterwards, a restriction digest using NcoI was performed to evaluate the purified plasmids. Sequences were then confirmed using either the Microsynth Sanger Sequencing service for regions up to 1000 base pairs or Plasmidsaurus Nanopore Sequencing for sequencing the whole plasmid.

Lentivirus production

24h before the experiment 0.9 mio HEK293T cells were seeded in a six-well plate. The following day 250 µL Gibco OptiMEM medium and 6 µL Mirus TransIT-293 Transfection reagent per well were incubated at room temperature for 15 minutes to allow the transfection reagent to form a lipid complex. Meanwhile, 1.5 µg of the plasmid of interest were mixed with 0.1 µg gag/pol, REV, and TAT packaging plasmids and 0.2 µg VSVG packaging plasmid (equivalent to 5 µL of the aliquoted packaging Master Mix). 256 µL of the lipid complex was then added to the plasmid mix and incubated for another 15 minutes, this was then added dropwise to the cells. 6 hours after the transfection the medium was changed. Lentiviral supernatant was collected after 24 and 48 hours or after 48 and 72 hours. The lentiviral supernatant was centrifuged for 5 minutes at 1000 ×g, then filtered through a 25 µm filter and shock-frozen in cryovials using liquid nitrogen.

Lentivirus transduction

0.2 mio. A549 cells were seeded in a six-well plate the day before the transduction. Medium was removed the following day and replaced by fresh medium with 50 % Lentiviral supernatant. To increase the efficiency of transduction 2 µL of polybrene were added. The cationic polymer reduces the surface repulsion between the cell

membrane and the virus which aids the virus in infecting the host cell. If the Lentivirus titer was suspected to be very low a “Spinfection” was performed, here the plate was centrifuged for 1 hour at 30 degrees Celsius at 1000 ×g after the transduction. About 48 h after the transduction cells having stably integrated the genes of interest were either selected with FACS or antibiotic treatment.

Puromycin selection

48 hours after Lentivirus transduction the antibiotic puromycin was added to the cell culture medium at a final concentration of 3 µg/mL. The medium was changed every two to three days and fresh puromycin was added until all the cells in the negative control were dead, which happened about 5 days after initial puromycin addition. The remaining cells were then cultured in DMEM+10 % FBS with either 1 µg/mL puromycin or none of the antibiotic.

Doxycycline treatment

A 1 mg/mL Doxycycline hyclate (Dox) solution was prepared by dissolving 1 mg of the antibiotic (purchased from Sigma Aldrich) in 1 mL of sterile water. 0.1mio. cells were seeded in a 12-well plate. The following day the Dox solution was added to the medium to achieve a final concentration of 0.1, 0.5 or 1 µg/mL. The medium was changed every day and fresh Doxycycline was added. Three days after the initial Dox addition the cells were split and half were harvested for Western blotting, the rest of the cells were incubated in fresh medium containing the corresponding Dox concentration. After five and seven days the cells were again harvested for immunoblotting. Additionally, cells were incubated in 1 µg/mL Dox for 24 hours to assess early response to the treatment.

Immunoblotting

Cells were washed with PBS and treated with trypsin for 5 minutes, which was then quenched with 4 times the amount of medium. The cell count was assessed with the Thermo Fisher Countess™ cell counter and the desired amount of cells was centrifuged at 1000 ×g for 5 minutes, the pellet was washed with PBS and centrifuged again for 5 minutes at 1000 ×g, the PBS was then aspirated. 100 µL lysis buffer (10 mM Tris/HCl pH 7.5, 150 mM NaCl, 0.5 mM EDTA, 0.5 % Nonidet P40 Substitute, 0.09 % sodium azide) plus 1 µL Halt™ Protease Inhibitor Cocktail (100X) were added to each sample, samples are then incubated for 1 hour at 4 degrees, they were then centrifuged at 20 000 ×g to remove cellular debris. Protein concentrations in the supernatant were assessed using the Pierce® Microplate BCA Protein Assay Kit. Then the corresponding amount of 4X NuPAGE™ sample buffer was added to the cell lysate. This was boiled for 10 minutes at 76 °C shaking at 500 rpm. Samples were loaded on SurePAGE™ Bis-Tris 4-20 % precast polyacrylamide gel together with PageRuler™ Plus Prestained Protein Ladder. Gel was run in 1X SDS Running buffer for 1 h at 150 V. Proteins were then transferred to a polyvinylidene fluoride (PVDF) membrane, which was activated in methanol. Transfer was performed at either 80 V for 4 hours or at 30 V overnight. Membrane was then washed three times with water and stained with Ponceau S to check if proteins were transferred. The stain was then removed with 0.1 % sodium hydroxide solution or just sterile water. The membrane was then blocked with 5 % milk powder in water for 1 hour, then washed three times with TBS-Tween. The membrane was incubated in primary antibody solution overnight, washed three times with TBS-T, and incubated in secondary antibody solution for 1-2 hours. Proteins were then detected with Pierce™ ECL Western Blotting Substrate reagents. Western blots were done using the anti-FLAG-M2 antibody, the anti-V5 antibody (Cell signaling, 13202), or the anti-ISG15 antibody (ThermoFisher, 7H29L24).

List of all primers

The following table includes all primer names, sequences, melting and annealing temperatures, which were calculated using the NEB Tm Calculator (tmcalculator.neb.com). All primers were used together with NEB Q5® High-Fidelity DNA Polymerase, except oMP0029 and oMP0030 which were used with *Taq* 2X Master Mix.

Table 5: List of all primers

Name	Purpose	Sequence	Tm (ºC)	Anneal at (ºC)
oMP0001	P2A top	TGGCAGCGGCGCCACCAACTTCTCCCTGCTGAAGCAGGCCGGCGACGTGGAGGAGAACCCCGGCCCCAT	96	72
oMP0002	P2A bottom	GGGGCCGGGGTTCTCCTCCACGTCGCCGGCCTGCTTCAGCAGGGAGAAGTTGGTGGCGCCGCTGCCAAT	95	72
oMP0003	Fragment 1 FW (V5-ISG)	TCTGGGACGTCGTATGGGTAGTTAATTAAGCCACCCCGCAG	79	72
oMP0004	Fragment 1 RV (V5-ISG)	TCAGATCGCCTGGAGAATTGGGGAAAGCCGATCC	79	72
oMP0005	Fragment 2 FW (UBA7)	CGGGGTGGCTTAATTAACTACCCATACGACGTCCCAGAC	78	72
oMP0006	Fragment 2 RV (UBA7)	AAAGGCGCAACCCCAACCCCGTGACAGGGTGG	84	72
oMP0007	Fragment 3 FW (PGK)	CAAGGCAGCCACCCTGTCACGGGGTTGGGGTTG	84	72
oMP0008	Fragment 3 RV (PGK)	AGCTCCTCGCCCTTGCTCACGGTGAATTGCTG	80	72

oMP0009	Fragment 4 FW (EGFP)	TCTCTCCCCAGCAATTCACCGTGAGCAAGGGC	80	72
oMP0010	Fragment 4 RV (EGFP)	AGCAACATAGTTAAGAATACGATCTTGTACAGCTCGTCC ATGCCGAG	77	72
oMP0013	Fragment 5 FW (UBE2L6)	TCCTCCGCGACCTCCGCTCCATGTTAATTAAGGAGGGC CGGTC	81	72
oMP0014	Fragment 5 RV (UBE2L6)	GTCAGATCGCCTGGAGAATTGGGACTACAAAGACGATG AC	77	72
oMP0015	Fragment 6 FW (Herc5)	CCGGCCCTCCTTAATTAACATGGAGCGGAGGTCGCG	76	72
oMP0016	Fragment 6 RV (Herc5)	TTAGTGGTGGTGGTGGTGGTGGAGCCAAATCCTCTGTT GTTGTTG	81	72
oMP0017	ISG-AA	TCTGGGACGTCGTATGGGTAGTTAATTAAGGCAGCCCG CAGGCGCAG	85	72
oMP0018	ISG no V5	TCAGATCGCCTGGAGAATTGGGGCTGGGACCTGACGG TGAAG	81	72
oMP0019	nested PCR FW (Herc5)	ATAGAATACAAGCTACTTGTTC	56	57
oMP0020	nested PCR RV (Herc5)	TCACTATAGTTCTAGAGGCTC	59	57
oMP0021	pro-ISG GG	AGATCTTCCTCCTGGTTCTGTTCCGCCACCCCGCAGG	84	72
oMP0022	pro-ISG AA	AGATCTTCCTCCTGGTTCTGTTCCGGCAGCCCGCAGG CGCAG	87	72

oMP0023	ISG15 Gibson	GTCGTATGGGTAGTTAATTAAAGATCTTCCTCCTGGTTCTGTTCC	74	72
oMP0024	Fragment 2 FW (UBA7) pro ISG	CAGAACCAGGAGGAAGATCTTTAATTAACTACCCATACGACGTCCCAGAC	77	72
oMP0025	NheI	GCTAGCCAATTCTCCAGGCGATCTGACG	75	69
oMP0026	EcoRV	ATCGTATTCTTAACTATGTTGCTCCTTTTACGC	68	69
oMP0027	AgeI	CCGGTCCACCACCACCACCACCACTAAG	79	69
oMP0029	Colony PCR FW	ATAAGCAGAGCTCGTTTAGTG	52	47
oMP0030	Colony PCR RV	TTCAGCAGGGAGAAGTTG	52	47
oMP0031	ISG P2A RV	CGCCGGCCTGCTTCAGCAGGGAGAAGTTGGTGGCGCCGCTGCCAGATCTTCCTCCTGG	92	72
oMP0032	UBA7 P2A FW	CTGCTGAAGCAGGCCGGCGACGTGGAGGAGAACCCCGGCCCCTACCCATACGACGTCC	92	72
oMP0033	Ube2L6 P2A FW	CGCCGGCCTGCTTCAGCAGGGAGAAGTTGGTGGCGCCGCTGCCGGAGGGCCGGTCCACTC	95	72
oMP0034	Herc5 P2A FW	CTGCTGAAGCAGGCCGGCGACGTGGAGGAGAACCCCGGCCCCATGGAGCGGAGGTCGCGG	95	72
oMP0035	TRIM25 nested FW	CAGCAGTTGTGTCCCGACC	69	68
oMP0036	TRIM25 nested RV	TCCCATGCTCCCAATCCTTG	67	68

oMP0037	TRIM25 Gibson FW	TGGAGGAGAACCCCGGCCCCATGGCAGAGCTGTGC	87	72
oMP0038	TRIM25 Gibson RV	GTGGTGGTGGTGGTGGTGGACTACTTGGGGGAGCAGA	84	72
oMP0040	Vector (TRIM25) RV	AGGGGGCACAGCTCTGCCATGGGGCCGGGGTT	89	72
oMP0041	ARIH1 nested FW	TCCGGACATCAGCCGGAG	70	68
oMP0042	ARIH1 nested RV	ACCAGTGGTGTCAGAATAGGC	67	68
oMP0043	ARIH1 Gibson FW	TGGAGGAGAACCCCGGCCCCATGGACTCGGACGAGG	87	72
oMP0044	ARIH1 Gibson RV	GTGGTGGTGGTGGTGGTGGATCAGTCCTCAATGTACTCCC	81	72
oMP0046	Vector (ARIH1) RV	TAGCCCTCGTCCGAGTCCATGGGGCCGGGGTT	86	72
oMP0047	ATG EGFP RV	TCCTCGCCCTTGCTCACCATGGTGAATTGCTG	79	72
oMP0048	ATG EGFP FW	TCTCTCCCCAGCAATTCACCATGGTGAGCAAGGGC	81	72
oMP0049	ATG V5 ISG	TCAGATCGCCTGGAGAATTGGACCATGGGAAAGCCGATCC	81	72
oMP0050	ATG ISG	TCAGATCGCCTGGAGAATTGGACCATGGGCTGGGACCTGACGGTGAAG	85	72

oMP0051	ATG Ube2L6	GTCAGATCGCCTGGAGAATTGGACCATGGACTACAAAG ACGATGAC	79	72
oMP0052	NheI kozak	CATGGTCCAATTCTCCAGGCGATCTGACG	74	72
oMP0053	GFP stop codon	AGCAACATAGTTAAGAATACGATCTTGTATTACAGCTCGT CCATGCCGAG	76	72
oMP0054	Herc5 his stop	TTAGTGGTGGTGGTGGTGGTGGCCAAATCCTCTGTTGTT GTTG	80	72
oMP0055	ARIH1 stop	GTGGTGGTGGTGGTGGTGGTCCTCAATGTACTCCC	81	72
oMP0056	TRIM25 stop	GTGGTGGTGGTGGTGGTGCTTGGGGGAGCAGA	84	72

List of engineered cell lines

The following table contains descriptions of all cell lines that were engineered during this project, all cell lines were derived from A549. Aliquots of these cells were frozen in cryovials (1 million cells per 1 mL of freezing mixture) and are stored in the -150 °C freezer in a box labeled “MP cells”. It is important to note that cell lines cMP001-4 do not contain the rtTA transactivator and will need to be transduced with the gene for this protein to enable expression of ISG15 and the E1 enzyme.

Table 6: List of engineered cell lines

Name	History	Description	Selection
cMP001	pMP001	V5-ISG15^{GG}-UBA7, **no** rtTA	GFP FACS
cMP002	pMP002	V5-ISG15^{AA}-UBA7, **no** rtTA	GFP FACS
cMP003	pMP003	ISG15^{GG}-UBA7, **no** rtTA	GFP FACS
cMP004	pMP004	ISG15^{AA}-UBA7, **no** rtTA	GFP FACS
cMP005	pMP005	UBE2L6-HERC5	Puromycin
cMP006	pMP006	UBE2L6-TRIM25	Puromycin
cMP007	cMP001, pMP005	V5-ISG15^{GG}-UBA7, UBE2L6-HERC5	GFP FACS then Puromycin
cMP008	cMP002+ pMP005	V5-ISG15^{AA}-UBA7, UBE2L6-HERC5	GFP FACS then Puromycin
cMP009	cMP003+ pMP005	ISG15^{GG}-UBA7, UBE2L6-HERC5	GFP FACS then Puromycin
cMP010	cMP004+ pMP005	ISG15^{AA}-UBA7, UBE2L6-HERC5	GFP FACS then Puromycin

cMP011	cMP001+ pMP006	V5-ISG15^{GG}-UBA7, UBE2L6-TRIM25	GFP FACS then Puromycin
cMP012	cMP002+ pMP006	V5-ISG15^{AA}-UBA7, UBE2L6-TRIM25	GFP FACS then Puromycin
cMP013	cMP003+ pMP006	ISG15^{GG}-UBA7, UBE2L6-TRIM25	GFP FACS then Puromycin
cMP014	cMP004+ pMP006	ISG15^{AA}-UBA7, UBE2L6-TRIM25	GFP FACS then Puromycin
cMP015	pMP005.1	UBE2L6-HERC5, His-tag **not** functional, **no** aliquots were frozen	Puromycin
cMP016	pMP006.1	UBE2L6-TRIM25, His-tag **not** functional, **no** aliquots were frozen	Puromycin
cMP017	cMP015+ pMP001	V5-ISG15^{GG}-UBA7, UBE2L6-HERC5, His-tag **not** functional	Puromycin then GFP FACS
cMP018	cMP015+ pMP002	V5-ISG15^{AA}-UBA7, UBE2L6-HERC5, His-tag **not** functional	Puromycin then GFP FACS
cMP019	cMP016+ pMP001	V5-ISG15^{GG}-UBA7, UBE2L6-TRIM25, His-tag **not** functional	Puromycin then GFP FACS
cMP020	cMP016+ pMP002	V5-ISG15^{AA}-UBA7, UBE2L6-TRIM25, His-tag **not** functional	Puromycin then GFP FACS

Discussion

In summary we were able to engineer cell lines that express all the components of the ISGylation machinery under an inducible promoter. This was achieved by cloning the coding regions of ISG15 and its three conjugating enzymes into a lentiviral vector. After the production of lentivirus, A549 cells were transduced with the two constructs sequentially and later selected. After selection via FACS or antibiotic treatment, cells were treated with Doxycycline to induce the expression of ISG15 and its conjugation machinery.

Although this reductionist approach of reconstituting the ISGylation machinery will enable us to investigate ISGylation separated from the Interferon response, this system does have some limitations. There are some concessions that were made for technical reasons that might have an impact on the function of the system, like ISG15 and the E1, as well as the E2 and E3 enzymes being connected by a 2A peptide. The co-translational cleavage of the peptide is never 100 % effective which means that there will likely be a low level of fusion proteins in the cell, depending on the baseline level of activity of the C-terminal processing protease. However, ISG15 is fused to UBA7 at the C-terminus which means that the conjugation site of ISG15 is eclipsed and the fusion protein will not be able to ISGylate other proteins. Another concern is that this may result in UBA7-derived peptides showing up in an ISG15 immunoprecipitation, mimicking a true biological interaction of these two proteins.

Another limitation of this system is that while HERC5 is only expressed after Interferon stimulation, this is not the case for the other two E3 enzymes TRIM25 and ARIH1. This means that these two enzymes will still be present and be able to ISGylate their substrates in the engineered cell lines. Although we are currently working on generating cell lines that contain knockouts of each of the E3 enzymes, which will enable us to investigate the target specificity of each of the enzymes. Keeping the limitations of the system in mind we believe that these engineered cell lines can be used to model and research the effects of ISGylation on the host proteome as well as the viral proteome during infection.

The problem with studying an antiviral defense mechanism like ISGylation is proposed to be, is that when it works well in hindering the replication of a virus then there will be few ISGylated viral proteins that can be detected as the abundance of the virus itself would be low. For this reason we hope that only expressing the ISGylation machinery without all other ISGs will make it possible to analyze ISGylated viral proteins via mass spectrometry. The V5 tag on ISG15 allows immunoprecipitation of ISGylated proteins with the robust and sensitive V5 antibody and subsequent analysis of the precipitated proteins via mass spectrometry.

We also want to see how ISGylation alone affects viral replication. Here the engineered cell lines would be infected with a virus such as Influenza B, a virus that can infect the epithelial lung cancer cells A549, which were used as the background cell line for this project. Furthermore, IBV infection leads to strong ISG15 induction and the virus has developed a strategy to inhibit ISGylation with its NS1 protein sequestering ISG15 and blocking its activation (Yuan et al., 2001). Using either a simple plaque assay or a fluorescently labeled virus we will be able to compare and quantify the replication of the virus in our engineered cells only expressing the ISGylation machinery upon pharmacological induction, wildtype cells, and cells that were treated with Interferon. This experiment will show to what extent ISGylation modulates the ability of host cells to fight viral infection.

These cell lines will not only be useful for finding ISGylated viral proteins but also for studying ISGylation of the host proteome isolated from the global Interferon response. We aim to understand the effects of ISGylation on abundance and localization of host proteins. To investigate this two experiments can be done, the first being a whole proteome mass spectrometry run, where induced cells will be compared to A549 that were treated with Dox for the same amount of time. This will show the differential regulation of proteins in the absence or presence of ISGylation.

In cellular responses to stressors for example a viral infection proteins are not only regulated by changes in abundance but also changes in localization. The different

compartments of a cell, which include the nucleus, organelles, and the cytoplasm can be separated by subcellular fractionation. This encompasses lysing the cells and then separating the compartments with a three-step centrifugation protocol developed by Hein et al. (2023). The spatial distribution of proteins in the different fractions can then be revealed by mass spectrometry. This will allow us to profile the effect ISG15 and ISGylation has on the localization of proteins in the cell.

Taken together, I have generated an important reagent that will enable the focused, reductionist investigation of the molecular consequences of ISGylation, disentangled from the Interferon response. This will help the community in advancing our understanding of this ubiquitous, yet functionally elusive post-translational modification.

Zusammenfassung

Die angeborene Immunantwort ist die erste Verteidigung einer Zelle im Kampf gegen Pathogene. Sobald der Krankheitserreger erkannt wird, signalisiert die Zelle mit Hilfe von Interferonen den benachbarten Zellen, dass sie bestimmte Gene transkribieren sollen. Eines der Gene, welches durch die Interferon-Reaktion Typ 1 am stärksten und schnellsten induziert wird, ist das Interferon-stimulierte Gen 15 (ISG15). Ähnlich wie bei der Ubiquitinierung erfordert die Konjugation von ISG15 an seine Zielproteine eine Kaskade von drei Enzymen (E1, E2, und E3).

Da ISG15 durch den Interferon-Signalweg produziert wird, wird vermutet, dass sowohl ISGylierung als auch ISG15 zur Abwehr einer Virusinfektion beitragen. Um die Auswirkungen der ISGylierung während einer Virusinfektion vollständig zu charakterisieren, ist es erforderlich, das gesamte Proteom zu betrachten. Des Weiteren beeinflusst ISGylierung zahlreiche Wirtsproteine, insbesondere jene, die als Reaktion auf die Interferon-Signalgebung produziert werden, dies stellt eine weitere Herausforderung dar.

Daher war es unser Ziel, ein System zu entwickeln, bei dem die ISGylierung von der globalen Interferon-Reaktion getrennt werden kann. Zuerst wurden Plasmide entwickelt, die die Sequenzen aller Komponenten wichtig für ISGylierung enthielten. Die Gene für ISG15 und die Enzyme E1, E2 und E3 wurden in lentivirale Vektoren geklont, die dann zur Erzeugung von Zelllinien verwendet wurden, diese Gene über das TetOn-System exprimieren. Wir konnten zeigen, dass die Interferon-Reaktion mit dem JAK-Inhibitor Ruxolitinib wirksam ausgeschaltet werden konnte. Diese Zelllinien können für die Analyse des gesamten Proteoms einer Zelle verwendet werden, um mehr Einblick in die Auswirkungen der ISGylierung auf das menschliche Proteom zu gewinnen, ohne von der Interferon-Reaktion beeinflusst zu werden.

References

Afsar, M., Liu, G., Jia, L., Ruben, E. A., Nayak, D., Sayyad, Z., Bury, P. D. S., Cano, K. E., Nayak, A., Zhao, X. R., Shukla, A., Sung, P., Wasmuth, E. V., Gack, M. U., & Olsen, S. K. (2023). Cryo-EM structures of Uba7 reveal the molecular basis for ISG15 activation and E1-E2 thioester transfer. Nature Communications, 14(1). https://doi.org/10.1038/s41467-023-39780-z

Ahler, E., Sullivan, W. J., Cass, A., Braas, D., York, A. G., Bensinger, S. J., Graeber, T. G., & Christofk, H. R. (2013). Doxycycline alters metabolism and proliferation of human cell lines. PLoS ONE, 8(5), https://doi.org/10.1371/journal.pone.0064561

Arimoto, K., Löchte, S., Stoner, S. A., Burkart, C., Zhang, Y., Miyauchi, S., Wilmes, S., Fan, J., Heinisch, J. J., Li, Z., Yan, M., Pellegrini, S., Colland, F., Piehler, J., & Zhang, D. (2017). STAT2 is an essential adaptor in USP18-mediated suppression of type I interferon signaling. Nature Structural & Molecular Biology, 24(3), 279–289. https://doi.org/10.1038/nsmb.3378

Bécares, M., Albert, M., Tárrega, C., Coloma, R., Falqui, M., Luhmann, E. K., Radoshevich, L., & Guerra, S. (2023). ISG15 is required for the dissemination of vaccinia virus extracellular virions. Microbiology Spectrum, 11(3). https://doi.org/10.1128/spectrum.04508-22

Bertram, R., & Hillen, W. (2007). The application of Tet repressor in prokaryotic gene regulation and expression. Microbial Biotechnology, 1(1), 2–16. https://doi.org/10.1111/j.1751-7915.2007.00001.x

Bogunovic, D., Boisson-Dupuis, S., & Casanova, J. (2013). ISG15: leading a double life as a secreted molecule. Experimental & Molecular Medicine, 45(4), e18. https://doi.org/10.1038/emm.2013.36

Bogunovic, D., Byun, M., Durfee, L. A., Abhyankar, A., Sanal, O., Mansouri, D., Salem, S., Radovanovic, I., Grant, A. V., Adimi, P., Mansouri, N., Okada, S., Bryant, V. L., Kong, X., Kreins, A., Velez, M. M., Boisson, B., Khalilzadeh, S., Ozcelik, U., Casanova, J. (2012). Mycobacterial Disease and Impaired IFN-γ Immunity in Humans with Inherited ISG15 Deficiency. Science, 337(6102), 1684–1688. https://doi.org/10.1126/science.1224026

Chu, L., Qian, L., Chen, Y., Duan, S., Ding, M., Sun, W., Meng, W., Zhu, J., Wang, Q., Hao, H., Wang, C., & Cui, S. (2024). HERC5-catalyzed ISGylation potentiates cGAS-mediated innate immunity. Cell Reports, 43(3), 113870. https://doi.org/10.1016/j.celrep.2024.113870

Dalskov, L., Gad, H. H., & Hartmann, R. (2023). Viral recognition and the antiviral interferon response. The EMBO Journal, 42(14). https://doi.org/10.15252/embj.2022112907

Das, A. T., Tenenbaum, L., & Berkhout, B. (2016). Tet-On systems for doxycycline-inducible gene expression. Current Gene Therapy, 16(3), 156–167. https://doi.org/10.2174/1566523216666160524144041

Dull, T., Zufferey, R., Kelly, M., Mandel, R. J., Nguyen, M., Trono, D., & Naldini, L. (1998). A Third-Generation Lentivirus Vector with a Conditional Packaging System. Journal of Virology, 72(11), 8463–8471. https://doi.org/10.1128/jvi.72.11.8463-8471.1998

Durfee, L. A., Lyon, N., Seo, K., & Huibregtse, J. M. (2010). The ISG15 conjugation system broadly targets newly synthesized proteins: Implications for the antiviral function of ISG15. Molecular Cell, 38(5), 722–732. https://doi.org/10.1016/j.molcel.2010.05.002

Dzimianski, J. V., Scholte, F. E., Bergeron, É., & Pegan, S. D. (2019). ISG15: It's complicated. Journal of Molecular Biology, 431(21), 4203–4216. https://doi.org/10.1016/j.jmb.2019.03.013

Gibson, D. G., Young, L., Chuang, R., Venter, J. C., Hutchison, C. A., & Smith, H. O. (2009). Enzymatic assembly of DNA molecules up to several hundred kilobases. Nature Methods, 6(5), 343–345. https://doi.org/10.1038/nmeth.1318

Gossen, M., & Bujard, H. (1992). Tight control of gene expression in mammalian cells by tetracycline-responsive promoters. PNAS, 89(12), 5547–5551. https://doi.org/10.1073/pnas.89.12.5547

Gossen, M., Freundlieb, S., Bender, G., Müller, G., Hillen, W., & Bujard, H. (1995). Transcriptional activation by tetracyclines in mammalian cells. Science, 268(5218), 1766–1769. https://doi.org/10.1126/science.7792603

Hein, M. Y., Peng, D., Todorova, V., McCarthy, F., Kim, K., Liu, C., Savy, L., Januel, C., Baltazar-Nunez, R., Bax, S., Vaid, S., Vangipuram, M., Ivanov, I. E., Byrum, J. R., Pradeep, S., Gonzalez, C. G., Aniseia, Y., Wang, E., Creery, J. S., Leonetti, M. D. (2023). Global organelle profiling reveals subcellular localization and remodeling at proteome scale. bioRxiv (Cold Spring Harbor Laboratory). https://doi.org/10.1101/2023.12.18.572249

Heinz, N., Hennig, K., & Loew, R. (2013). Graded or threshold response of the tet-controlled gene expression: all depends on the concentration of the transactivator. BMC Biotechnology, 13(1). https://doi.org/10.1186/1472-6750-13-5

Invivogen. (2023). Ruxolitinib [Adventure; E-book: PDF]. https://www.invivogen.com/sites/default/files/invivogen/products/files/ruxolitinib_tds.pdf

Kallunki, T., Barisic, M., Jäättelä, M., & Liu, B. (2019). How to choose the right inducible gene expression system for mammalian studies? Cells, 8(8), 796. https://doi.org/10.3390/cells8080796

Kang, J. A., Kim, Y. J., & Jeon, Y. J. (2022). The diverse repertoire of ISG15: more intricate than initially thought. Experimental & Molecular Medicine, 54(11), 1779–1792. https://doi.org/10.1038/s12276-022-00872-3

Kennedy, M. A., Tyl, M. D., Betsinger, C. N., Federspiel, J. D., Sheng, X., Arbuckle, J. H., Kristie, T. M., & Cristea, I. M. (2022). A TRUSTED targeted mass spectrometry assay for

pan-herpesvirus protein detection. Cell Reports, 39(6), 110810. https://doi.org/10.1016/j.celrep.2022.110810

Liu, Z., Chen, O., Wall, J. B. J., Zheng, M., Zhou, Y., Wang, L., Vaseghi, H. R., Qian, L., & Liu, J. (2017). Systematic comparison of 2A peptides for cloning multi-genes in a polycistronic vector. Scientific Reports, 7(1). https://doi.org/10.1038/s41598-017-02460-2

Martin-Fernandez, M., García-Morato, M. B., Gruber, C., Loza, S. M., Malik, M. N. H., Alsohime, F., Alakeel, A., Valdez, R., Buta, S., Buda, G., Marti, M. A., Larralde, M., Boisson, B., Rodriguez, M. F., Qiu, X., Chrabieh, M., Ayed, M. A., Muhsen, S. A., Desai, J. V., Bogunovic, D. (2020). Systemic type I IFN inflammation in human ISG15 deficiency leads to necrotizing skin lesions. Cell Reports, 31(6), 107633. https://doi.org/10.1016/j.celrep.2020.107633

Mirzalieva, O., Juncker, M., Schwartzenburg, J., & Desai, S. (2022). ISG15 and ISGylation in human diseases. Cells, 11(3), 538. https://doi.org/10.3390/cells11030538

Nakashima, H., Nguyen, T., Goins, W. F., & Chiocca, E. A. (2015). Interferon-stimulated Gene 15 (ISG15) and ISG15-linked Proteins Can Associate with Members of the Selective Autophagic Process, Histone Deacetylase 6 (HDAC6) and SQSTM1/p62. Journal of Biological Chemistry, 290(3), 1485–1495. https://doi.org/10.1074/jbc.m114.593871

Narasimhan, J., Wang, M., Fu, Z., Klein, J. M., Haas, A. L., & Kim, J. P. (2005). Crystal structure of the interferon-induced ubiquitin-like protein ISG15. Journal of Biological Chemistry, 280(29), 27356–27365. https://doi.org/10.1074/jbc.m502814200

Okumura, A., Pitha, P. M., & Harty, R. N. (2008). ISG15 inhibits Ebola VP40 VLP budding in an L-domain-dependent manner by blocking Nedd4 ligase activity. PNAS, 105(10), 3974–3979. https://doi.org/10.1073/pnas.0710629105

Ostojic, A., Vrhovac, R., & Verstovsek, S. (2011). Ruxolitinib: a new JAK1/2 inhibitor that offers promising options for treatment of myelofibrosis. Future Oncology, 7(9), 1035–1043. https://doi.org/10.2217/fon.11.81

Peng, Q., Li, G., Sun, W., Yang, J., Quan, G., & Liu, N. (2016). Analysis of ISG15-Modified Proteins from A549 Cells in Response to Influenza Virus Infection by Liquid Chromatography-Tandem Mass Spectrometry. CHINESE JOURNAL OF ANALYTICAL CHEMISTRY (CHINESE VERSION), 44(6), 850–856. https://doi.org/10.1016/s1872-2040(16)60936-2

Perng, Y., & Lenschow, D. J. (2018). ISG15 in antiviral immunity and beyond. Nature Reviews Microbiology, 16(7), 423–439. https://doi.org/10.1038/s41579-018-0020-5

Pinto-Fernandez, A., Salio, M., Partridge, T., Chen, J., Vere, G., Greenwood, H., Olie, C. S., Damianou, A., Scott, H. C., Pegg, H. J., Chiarenza, A., Díaz-Saez, L., Smith, P., Gonzalez-Lopez, C., Patel, B., Anderton, E., Jones, N., Hammonds, T. R., Huber, K.,Kessler, B. M. (2020). Deletion of the deISGylating enzyme USP18 enhances tumour cell antigenicity

and radiosensitivity. British Journal of Cancer, 124(4), 817–830. https://doi.org/10.1038/s41416-020-01167-y

Platanitis, E., Demiroz, D., Schneller, A., Fischer, K., Capelle, C., Hartl, M., Gossenreiter, T., Müller, M., Novatchkova, M., & Decker, T. (2019). A molecular switch from STAT2-IRF9 to ISGF3 underlies interferon-induced gene transcription. Nature Communications, 10(1). https://doi.org/10.1038/s41467-019-10970-y

Potter, J. L., Narasimhan, J., Mende-Mueller, L., & Haas, A. L. (1999). Precursor processing of Pro-ISG15/UCRP, an interferon-B-induced ubiquitin-like protein. Journal of Biological Chemistry, 274(35), 25061–25068. https://doi.org/10.1074/jbc.274.35.25061

Qin, Y., Wang, M., Meng, X., Wang, M., Jiang, H., Gao, Y., Li, J., Zhao, C., Han, C., Zhao, W., & Zheng, X. (2024). ISGylation by HERCs facilitates STING activation. Cell Reports, 43(5), 114135. https://doi.org/10.1016/j.celrep.2024.114135

Quintás-Cardama, A., Vaddi, K., Liu, P., Manshouri, T., Li, J., Scherle, P. A., Caulder, E., Wen, X., Li, Y., Waeltz, P., Rupar, M., Burn, T., Lo, Y., Kelley, J., Covington, M., Shepard, S., Rodgers, J. D., Haley, P., Kantarjian, H.,Verstovsek, S. (2010). Preclinical characterization of the selective JAK1/2 inhibitor INCB018424: therapeutic implications for the treatment of myeloproliferative neoplasms. Blood, 115(15), 3109–3117. https://doi.org/10.1182/blood-2009-04-214957

Rossi, F. M., & Blau, H. M. (1998). Recent advances in inducible gene expression systems. Current Opinion in Biotechnology, 9(5), 451–456. https://doi.org/10.1016/s0958-1669(98)80028-1

Sandy, Z., Da Costa, I. C., & Schmidt, C. K. (2020). More than Meets the ISG15: Emerging Roles in the DNA Damage Response and Beyond. Biomolecules, 10(11), 1557. https://doi.org/10.3390/biom10111557

Shin, D., Mukherjee, R., Grewe, D., Bojkova, D., Baek, K., Bhattacharya, A., Schulz, L., Widera, M., Mehdipour, A. R., Tascher, G., Geurink, P. P., Wilhelm, A., Van Der Heden Van Noort, G. J., Ovaa, H., Müller, S., Knobeloch, K., Rajalingam, K., Schulman, B. A., Cinatl, J., Dikic, I. (2020). Papain-like protease regulates SARS-CoV-2 viral spread and innate immunity. Nature, 587(7835), 657–662. https://doi.org/10.1038/s41586-020-2601-5

Speer, S. D., Li, Z., Buta, S., Payelle-Brogard, B., Qian, L., Vigant, F., Rubino, E., Gardner, T. J., Wedeking, T., Hermann, M., Duehr, J., Sanal, O., Tezcan, I., Mansouri, N., Tabarsi, P., Mansouri, D., Francois-Newton, V., Daussy, C. F., Rodriguez, M. R., Bogunovic, D. (2016). ISG15 deficiency and increased viral resistance in humans but not mice. Nature Communications, 7(1). https://doi.org/10.1038/ncomms11496

Stieger, K., Belbellaa, B., Guiner, C. L., Moullier, P., & Rolling, F. (2009). In vivo gene regulation using tetracycline-regulatable systems. Advanced Drug Delivery Reviews, 61(7–8), 527–541. https://doi.org/10.1016/j.addr.2008.12.016

Thery, F., Eggermont, D., & Impens, F. (2021). Proteomics Mapping of the ISGylation landscape in innate immunity. Frontiers in Immunology, 12. https://doi.org/10.3389/fimmu.2021.720765

Thoresen, D., Wang, W., Galls, D., Guo, R., Xu, L., & Pyle, A. M. (2021). The molecular mechanism of RIG-I activation and signaling. Immunological Reviews, 304(1), 154–168. https://doi.org/10.1111/imr.13022

Woods, M. W., Kelly, J. N., Hattlmann, C. J., Tong, J. G. K., Xu, L. S., Coleman, M. D., Quest, G. R., Smiley, J. R., & Barr, S. D. (2011). Human HERC5 restricts an early stage of HIV-1 assembly by a mechanism correlating with the ISGylation of Gag. Retrovirology, 8(1). https://doi.org/10.1186/1742-4690-8-95

Wu, S., Xia, L., Shi, X., Dai, Y., Zhang, W., Zhao, J., Zhang, W., Weng, X., Lu, J., Le, H., Tao, S., Zhu, J., Chen, Z., Wang, Y., & Chen, S. (2020). RIG-I regulates myeloid differentiation by promoting TRIM25-mediated ISGylation. PNAS, 117(25), 14395–14404. https://doi.org/10.1073/pnas.1918596117

Xiong, T., Wei, M., Li, F., Shi, M., Gan, H., Tang, Z., Dong, H., Liuyu, T., Gao, P., Zhong, B., Zhang, Z., & Lin, D. (2022). The E3 ubiquitin ligase ARIH1 promotes antiviral immunity and autoimmunity by inducing mono-ISGylation and oligomerization of cGAS. Nature Communications, 13(1). https://doi.org/10.1038/s41467-022-33671-5

Yuan, W., Krug, R. M., & Institute for Cellular and Molecular Biology, Section of Molecular Genetics and Microbiology, University of Texas at Austin. (2001). Influenza B virus NS1 protein inhibits conjugation of the interferon (IFN)-induced ubiquitin-like ISG15 protein. In The EMBO Journal (Vols. 20–20, Issue 3, pp. 362–371). https://www.ncbi.nlm.nih.gov/pmc/articles/PMC133459/pdf/cde033.pdf

Zhang, X., Bogunovic, D., Payelle-Brogard, B., Francois-Newton, V., Speer, S. D., Yuan, C., Volpi, S., Li, Z., Sanal, O., Mansouri, D., Tezcan, I., Rice, G. I., Chen, C., Mansouri, N., Mahdaviani, S. A., Itan, Y., Boisson, B., Okada, S., Zeng, L., Pellegrini, S. (2014). Human intracellular ISG15 prevents interferon-α/β over-amplification and auto-inflammation. Nature, 517(7532), 89–93. https://doi.org/10.1038/nature13801

Zhao, C., Denison, C., Huibregtse, J. M., Gygi, S., & Krug, R. M. (2005). Human ISG15 conjugation targets both IFN-induced and constitutively expressed proteins functioning in diverse cellular pathways. PNAS, 102(29), 10200–10205. https://doi.org/10.1073/pnas.0504754102

Zhao, C., Hsiang, T., Kuo, R., & Krug, R. M. (2010). ISG15 conjugation system targets the viral NS1 protein in influenza A virus–infected cells. PNAS, 107(5), 2253–2258. https://doi.org/10.1073/pnas.0909144107

Zhao, C., Sridharan, H., Chen, R., Baker, D. P., Wang, S., & Krug, R. M. (2016). Influenza B virus non-structural protein 1 counteracts ISG15 antiviral activity by sequestering ISGylated viral proteins. Nature Communications, 7(1). https://doi.org/10.1038/ncomms12754